

Deep Learning Approach to Nailfold Capillaroscopy Based Diabetes Mellitus Detection

<https://doi.org/10.3991/ijoe.v18i06.27385>

Suma K V^(✉), S Sethu Selvi, Pranav Nanda, Manisha Shetty,
Vikas M, Kushagra Awasthi
Department of Electronics and Communication, Ramaiah Institute of Technology,
Bangalore, India
sumakv@msrit.edu

Abstract—Diabetes mellitus is a commonly occurring chronic metabolic disorder which has affected almost 400 million people around the world. It can lead to vascular structure alterations and various renal, cardiovascular, and neurological complications claiming numerous lives. Since diabetes mellitus results in vascular structure changes, Nailfold Capillaroscopy (NFC) based approach can be employed for the detection of diabetes. NFC is an inexpensive, non-invasive method which involves acquisition of images of capillaries in the nail bed region using a USB digital microscope, which is a novel and economical approach suitable for developing countries like India. Qualitative parameters of the capillaries such as tortuosity, hemorrhages, angiogenesis, elongated capillaries and quantitative parameters like length, width and mean capillary density are considered for diabetes detection. About 600 capillary images of healthy and diabetic subjects were collected and further data augmentation was performed to increase this to 1018 images dataset. This paper focuses on using NFC to obtain capillary images and employ deep learning-based object detection algorithm to localize these capillary loops on the nailbed and differentiate them into five classes namely, normal, wide, elongated, tortuosity and hemorrhages. This classification is of prominent significance to medical practitioners as this helps in gauging the severity and progression of the disorder.

Keywords—nailfold capillaroscopy, object detection, diabetes mellitus, capillary features, YOLO architecture

1. Introduction

Nailfold capillaroscopy (NFC) is a simple, non-invasive, and inexpensive approach that has a wide and immense potential as a medium of clinical aid in the field of medicine and research. NFC can be used in the diagnosis and prognosis of a spectrum of diseases such as diabetes, Rheumatoid Arthritis (RA), hypertension and Raynaud's disease. These disorders exhibit a chronic hyperglycemic state with the development of vascular structure alterations. Capillaries, in human physiology, are the minute blood vessels that are only one cell thick. They form networks throughout the tissues of the body where transfer of oxygen, carbon-di-oxide and other nutrients take place between

the bloodstream and the tissues. Their presence in the nail bed region in the finger appears parallel to the skin which can be imaged conveniently using a simple USB digital microscope, for the study of its morphology and microcirculation.

Diabetes is a commonly occurring chronic metabolic disorder which has affected almost 400 million people around the world. This leads to vascular structure alterations and various long-term renal, cardiovascular and neurological complications claiming several lives. Normally, the nailfold capillaries are arranged regularly and uniformly with hairpin like structure. But diabetic patients exhibit certain micro vascular and structural changes which are assessed quantitatively and qualitatively. Mean capillary density, length of capillary, and loop diameter are the quantitative features observed in diabetic patients. Qualitative parameters include tortuosity, which refers to the twisting or bending of capillaries, micro-hemorrhages, and avascular areas which is absence of two or more adjacent capillaries from the distal most rows. The acquisition of quantitative and qualitative parameters and their scoring plays significant roles to aid doctors in evaluating the severity and predicting the possible course of the disease.

The paper is organized as follows: Section 2 briefs on the existing NFC based algorithms. Section 3 elaborates on the proposed algorithm for diabetes detection using NFC. Section 4 presents the results and discussion. The paper is concluded, and future possible work is detailed in Section 5.

2. Existing algorithms

In [1] a review is provided which describes the method of capillaroscopy and emphasizes its usefulness in the evaluation of vascular micro architecture in patients with diabetes mellitus and its relation to its complications. The various studies conclude that capillaroscopy is capable of providing key data for detecting vascular characteristics in diabetic patients and thus, allows evaluating the progression of this disorder, making this a very potential future utility for diabetic detection. The authors in [2] describe and quantify NFC changes in Type 2 Diabetes Mellitus (T2DM). NFC images were captured for 10 fingernails for 96 patients with T2DM and 40 healthy normal subjects. The diabetics were subdivided into two groups: Group 1 – 46 patients with microvascular complications, Group 2 – 50 patients without any. The observations are 80.2% (77/96) of the patients with T2DM showed NFC changes as compared to 12.5% of the healthy subjects. NFC changes observed were unique morphological alterations like angulated and receding capillaries. Mean capillary density was reduced in Group 1 (6.57 ± 1.02 capillary/mm) as compared to Group 2 (7.03 ± 1.09 capillary/mm) with a p -value of 0.67 through Fisher's exact test. The difference due to quantitative analysis is not statistically significant as $p > 0.05$. 89.13% of Group 1 patients had NFC changes as compared to 72% in Group 2 with $p = 0.035$. Specific morphological changes were also significantly more common in Group 1 than Group 2, including tortuosity ($p = 0.035$), meandering capillaries ($p = 0.004$), capillary dropouts ($p = 0.012$), and bizarre capillaries ($p = 0.002$). The study suggests that NFC changes are correlated with qualitative features or microvascular complications in type 2 diabetics, possibly helping in noninvasive identification of patients at risk.

The objective of the paper [3] is to evaluate nailfold capillaries in T2DM patients and to determine the association of retinopathy with changes in the nailfold capillaries using high quality video capillaroscopy (NVC). Capillaroscopic findings and fundoscopic examinations were assessed in 216 patients with T2DM and 101 healthy subjects. Retinopathy was detected in 93 out of 216 diabetic patients (43.05%) while, capillaroscopic findings including tortuosity ($p < 0.001$), bushy capillary ($p < 0.001$), neoformation ($p < 0.001$), bizarre capillary ($p < 0.001$), micro-hemorrhage ($p = 0.001$), capillary ectasia ($p = 0.002$), and aneurysm ($p = 0.004$) were significantly higher in diabetic group than normal group. In logistic regression analysis, only tortuosity was shown significant with odds ratio of 2.106 ($p = 0.036$). The authors confirmed a significant relation between diabetes duration and most of the capillaroscopic findings and concluded that capillaroscopic changes were found to be correlated with diabetic retinopathy, in particular with longer disease duration. Capillaroscopic imaging could be a useful approach for assessment of diabetic microvascular changes.

The authors of [4] describe a fully automated system for extracting quantitative biomarkers from capillaroscopy images, using a layered machine learning approach. On an unseen set of 455 images, the proposed system detects and locates individual capillaries and makes measurements of vessel morphology that reveal statistically significant differences between patients with relatively benign primary Raynaud's phenomenon (RP), and those with potentially life-threatening systemic sclerosis (SSc). Distributions of capillary measurements – capillary density, median width and median tortuosity for the three groups: 104 images of healthy control (HC), 83 images of RP, and 268 images of SSc were considered. Tests for all measurements between all groups showed significant differences at 0.01 confidence level.

The proposed method in [5] emphasizes on the importance of USB digital microscope which is a cheaper alternative to commercially available expensive video capillaroscope which can render high quality images. As identifying anomalies in nailfold capillaries is a tedious and time-consuming process, this paper proposes an automated system to diagnose anomalies. The pre-processed nailfold capillary images are used for training machine learning models like logistic regression, fully connected neural network, Convolutional Neural Networks (CNN) [6, 7] and Random Forests. The performance was compared in terms of classification accuracy, sensitivity and specificity. The results prove logistic regression to be most accurate with a low classification error rate of 10.64%. while, a substantial classification accuracy of 72% was obtained with a small dataset by using bottleneck features of a deep CNN.

3. Methodology

The proposed algorithm employs the NFC approach in which nailfold images are captured through a USB digital microscope which is inexpensive in comparison to video capillaroscopy (NVC). This is a novel and an economically viable field of exploration especially in developing countries like India. The USB digital microscope used is AGPtek iT33 with magnification of 20X to 200X with a resolution of 640 x 480 ($\approx 2\mu\text{m}/\text{pixel}$) and it costs around USD \$29. When compared to other commonly used

devices for viewing capillaries, this device is extremely cost-effective but with lower image quality. The cost and specifications of other devices are listed below for comparison.

- Video Capillaroscopy (gold standard) has a magnification of 420X and resolution of $1\mu\text{m}/\text{pixel}$ with an approximate cost of USD \$3,000
- In a Stereomicroscope, panoramic NFC is possible with magnification ranging from 10X to 50X and resolution is about $4\mu\text{m}/\text{pixel}$. The cost ranges from USD \$200 to more than \$2,000.

The methodology consists of a deep learning-based object detection approach to individually label the capillaries into five distinct classes and further obtain quantitative parameters like length, width, capillary density etc.

Classification of the capillaries and acquisition of quantitative parameters, including other qualitative features like tortuosity, avascularity etc., is of very crucial significance to doctors to gauge severity of disease. Object detection algorithm is used for measuring quantitative features which humans cannot do with the naked eye. This localizes capillary loops on the nailbed and classifies them into five broad classes namely, “Normal”, “Wide”, “Elongated”, “Tortuosity”, and “Hemorrhages”. The criteria for classification of capillaries stems from Table 1 prepared in consultation with clinicians where the dimensions for each class is specified.

“Normal” class is not tabulated in Table 1. This new class was added by combining two classes “Rarefaction” and “Avascularity”, as these classes are not features of capillaries per se, but the description of lack of capillaries. The features of “Normal” class together with the remaining four classes describe the total number of capillaries in an NFC image. Capillary density is determined through “Normal”, “Wide”, “Elongated”, “Tortuosity”, and “Hemorrhages” classes. To account for “Avascularity” the distances between all consecutive capillaries is measured and compared against a threshold of $500\mu\text{m}$. Following are the steps involved in the proposed algorithm:

1. Training and test datasets are created
2. Deep learning architecture-based object detection algorithm is implemented
3. Detector algorithm is trained, and performance is evaluated
4. Capillaries are detected and features are extracted on-chip
5. The features are combined using a mathematical model to detect diabetes

Table 1. Criteria for classification of the capillaries

Sl. No.	Abnormality	Grade	Score	Criteria
1.	Rarefaction (R)	Absent	0	Capillary density: > 9
		Mild	1	Capillary density: > 7 and < 9
		Moderate	2	Capillary density: > 4 and < 7
		Severe	3	Capillary density: < 4
2.	Avascularity (A)	Absent	0	Distance between adjacent capillaries < 500µm
		Mild	1	Number of avascular regions = 1
		Moderate	2	Number of avascular regions = 2
		Severe	3	Number of avascular regions > 2
3.	Tortuosity (T)	Absent	0	Capillary loop width: < 50µm
		Mild	1	Number of capillaries with bushy appearance = 1
		Moderate	2	Number of capillaries with bushy appearance = 2
		Severe	3	Number of capillaries with bushy appearance > 2
4.	Hemorrhages (H)	Absent	0	Number of micro-hemorrhage clusters = 0
		Mild	1	Number of micro-hemorrhage clusters = 1
		Moderate	2	Number of micro-hemorrhage clusters = 2
		Severe	3	Number of micro-hemorrhage clusters > 2
5.	Elongated (E)	Absent	0	Capillary height: 96µm – 295µm
		Mild	1	Height of one capillary: > 300µm or < 96µm
		Moderate	2	Height of two capillaries: > 300µm or < 96µm
		Severe	3	Height of more than two capillaries: > 300µm or < 96µm
6.	Wide (W)	Absent	0	Capillary loop width: < 50µm
		Mild	1	Number of enlarged capillaries = 1
		Moderate	2	Number of enlarged capillaries = 2
		Severe	3	Number of enlarged capillaries > 2

3.1 Creation of training and test datasets

The first step in creating a dataset for object detection is labeling of images. A set of 600 images from both healthy and diabetic subjects were collected and capillaries were labeled using the scoring rules in Table 1. This constitutes the training dataset. Another similar set of 230 images were labeled and used as the test dataset. All images are of size 480 × 640.

Data augmentation was performed on the training set by the following random transformations as shown in Figure 1:

- Color jitter augmentation in HSV space (Contrast, Hue, Saturation and Brightness)
- Random horizontal or vertical flip

Transformation by scaling of images was not performed to preserve the original dimensions of the image as it is crucial in determining some of the classes of capillaries. Data augmentation is used to improve network accuracy by randomly transforming the

original data during training. The process is completely automatic (done internally by MATLAB) and each image, before being passed through the network, produces four other augmented images. Each image undergoes a random combination of horizontal flips and modified hue, saturation and brightness values. Along with the images the bounding boxes created through the labeling process is to be augmented correspondingly. Data augmentation is not applied to the test dataset as it is representative of the original image and was left unmodified for unbiased evaluation.

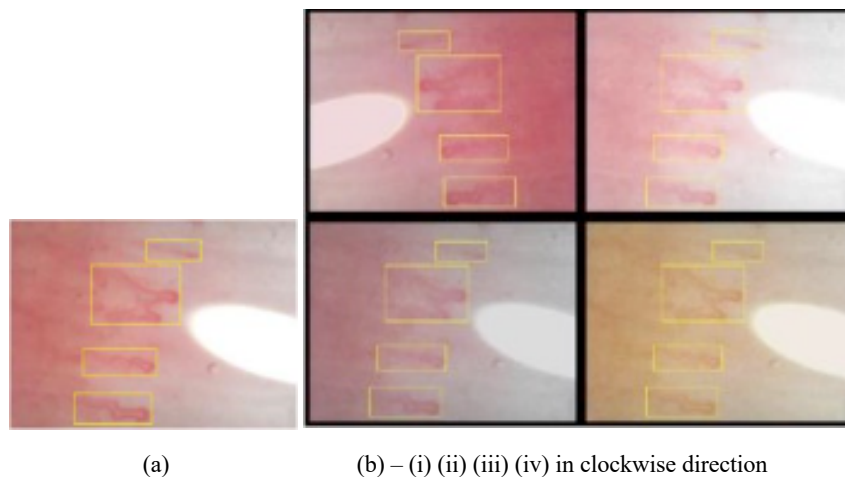


Fig. 1. (a) Original image with bounding boxes (b – i) Horizontal flip + increased saturation (b – ii) No flip + reduced contrast (b – iii) No flip + greyish hue (b – iv) no flip + yellowish hue

3.2 Deep learning architecture-based object detection

Two different networks YOLOv2 and YOLOv3 based on You Only Look Once (YOLO) architecture was considered for object detection and each network was trained on both the training set and augmented training set. The architecture of these networks is shown in Figure 2.

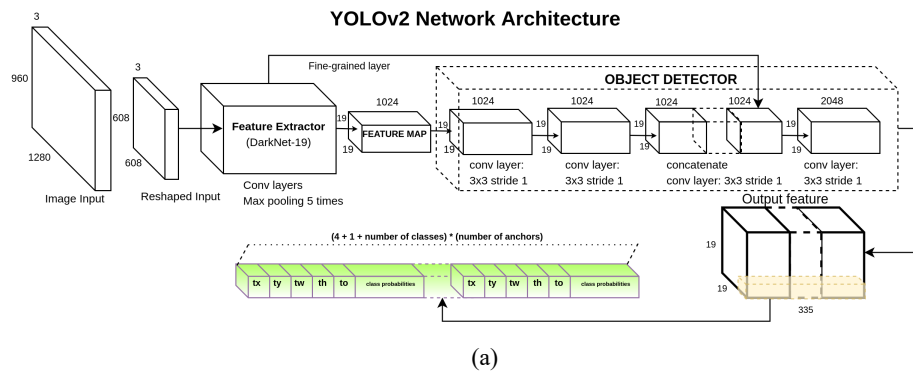
YOLOv2, also known as YOLO9000 [8] is a state-of-the-art, real-time object detection system that can detect over 9000 object categories. At 40fps, this algorithm provides 78.6% mean average precision, outperforming state-of-the-art methods like Faster RCNN with ResNet and SSD while still running significantly faster. It also provides a mean average precision of 19.7% on the ImageNet detection validation set.

A YOLOv2 network based on Darknet-19 classification network is composed of two subnetworks: feature extraction network, detection network. The original YOLO trains the classifier network and increases the resolution for detection and the network simultaneously switches to learning object detection by adjusting to the new input resolution. For YOLOv2 the feature extraction network is fine-tuned at the full resolution which gives the network time to adjust its filters to work better on higher resolution input. Then the resulting network is fine-tuned on detection. The feature extraction network

is typically a pre-trained convolution neural network (CNN) such as ResNet50, ResNet18 or MobileNetv2. The detection network is a small CNN compared to the feature extraction network and is composed of a few convolutional layers and layers specific to YOLOv2. This network requires four input parameters namely network input size, anchor boxes, feature extraction network and detection network as shown in Figure 2(a). The object detector part of the network obtains the input from the feature extraction part of the network. As in Figure 2(a), there are 3×3 and 1×1 convolution layers and down-sampling by a factor of 4 is used for feature extraction. The final part of Figure 2(a) conducts the same operations, but the down-sampling factor is 2 to keep the feature maps of these layers the same. Then, the local features are fused with the global features of one layer, which enhances local information and aids in distinguishing small differences. This modified YOLO which is YOLOv2 performs detection on a 13×13 feature map. For finer grained features of smaller objects, a pass through a layer that brings features from 26×26 resolution is added. This layer concatenates the higher resolution features with the low resolution features by stacking adjacent features into different channels instead of spatial locations.

The YOLOv3 [9] algorithm first separates an image into a grid and some number of anchor boxes are predicted around objects that score highly with the predefined classes. The boundary boxes are generated by clustering the dimensions of the ground truth boxes from the original dataset to find the most common shapes and sizes. However, unlike systems like Region-based CNN (R-CNN) and Fast R-CNN, YOLO is trained to do classification and bounding box regression at the same time.

This network is a hybrid approach between the network used in YOLOv2, Darknet-19, and a residual network. This uses 53 convolutional layers of successive 3×3 and 1×1 layers. The YOLOv3 detector is based on SqueezeNet and uses the feature extraction network with addition of two detection heads at the end. The second detection head is twice the size of the first detection head, so it is capable to detect small objects such as micro-hemorrhages and shortened capillaries. This detector uses anchor boxes estimated using training dataset to have better initial priors corresponding to the type of dataset and helps the detector learn to predict the boxes accurately. The architecture is illustrated in Figure 2(b).



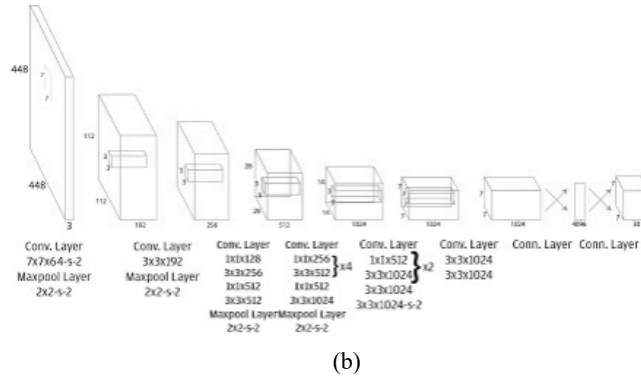


Fig. 2. Architecture of (a) YOLOv2 (b) YOLOv3

3.3 Training the detector algorithm

Initially, augmented training and test datasets were pre-processed to provide suitable inputs to the network architecture. All images together with their bounding boxes were resized to either $224 \times 224 \times 3$ or $227 \times 227 \times 3$ and pixel values were normalized to one.

Anchor boxes were estimated by using 7 anchors to achieve a good trade-off between number of anchors and mean intersection of union (IoU). A mean IoU greater than 0.5 is desirable. Although the images are resized which affects the capillary features, they are up-sampled back to original dimensions once the training and detection are completed. Seven anchor boxes were estimated, and the mean intersection of union (IoU) obtained is 0.71.

Several parameters such as mini-batch size, epochs, learning rate, regularization, and optimizer need to be specified for training. The parameters are listed in Table 2. Generally, a small mini-batch size with larger number of epochs (around 100 to 200) is required to satisfactorily train the model for good performance. The predicted bounding boxes on the test dataset are classified, labeled and capillary features are measured. These predicted boxes are compared with the ground truth boxes of the test dataset and detection performance for each of the 5 classes is calculated.

As in the case of any medical data the standard metric used to evaluate the performance are sensitivity (recall) and specificity (precision). A precision-recall curve for each of the 5 classes of capillaries is analyzed on the test dataset. This curve depicts precision at a particular level of recall. Ideally, recall should be as high as possible, which indicates that no capillaries are left undetected, and the operating point is set at the highest feasible value of recall so that the corresponding precision is not too low either. There is always a trade-off between precision and recall.

Table 2. Training algorithm parameter settings

Sl. No.	Parameter	Values
1.	Image input	227 × 227 × 3 images
2.	Batch size	16
3.	Number of epochs	200
4.	Regularization parameter	0.001
5.	Optimization algorithm	Stochastic gradient descent with momentum (SGDM)
6.	Step size	0.001
7.	Convolution	3 × 3 × 3 convolution, stride [2 2], zero padding
8.	Non-linearity	ReLU
9.	Pooling	3 × 3 Max pooling, stride [2 2], zero padding
10.	Concatenation	Depth concatenation of 2 inputs
11.	Normalization	Batch normalization with 256 channels
12.	Squeeze	1 × 1 × 28 convolution, stride [1 1], zero padding
13.	Expand (1 × 1)	1 × 1 × 32 convolution, stride [1 1], zero padding
14.	Expand (3 × 3)	3 × 3 × 32 convolution, stride [1 1], ones padding

3.4 Detection of capillaries and feature extraction

The final step is to test the deep learning model on unseen NFC based capillary images not part of the test dataset such as images from a real-time clinic scenario. Care must be taken during image acquisition to properly align the capillaries as far as possible in a horizontal position, as the bounding boxes are rectangles. The object detectors are implemented on NVIDIA GPUs such as Jetson Nano boards for real time inferencing. This requires additional peripherals such as an LED display and a user interface.

3.5 Mathematical model for combining features to detect diabetes

A mathematical relation between input variables shown in Table 1 namely R , A , T , H , E and W is derived to gives an output differentiating normal and diabetic images as in (1):

$$U = fn(R, A, T, H, E, W) \tag{1}$$

where R indicates Rarefaction, A indicates Avascularity, T indicates Tortuosity, H indicates Hemorrhages, E is the Elongation and W is Wide capillaries, with the output $\Psi_U(I) \in \{\text{normal, diabetic}\}$ which is a function fn of the input variables.

Each of the six features is defined with a set of scores from 0 to 3. The exponential expression does not support the variable value of zero. Hence the scores are incremented by 1 to obtain scores from 1 to 4 which results in $\Psi(I) \in \{1, 2, 3, 4\}$ for all the features. The exponential relation between the output and input variables is given by (2):

$$U = a.R^b.A^c.T^d.H^e.E^f.W^g \tag{2}$$

where a is the coefficient and b, c, d, e, f and g are the exponents of the input variables. The values of these coefficients are evaluated by framing seven equations which are derived from the training dataset. The derived values of the coefficient and exponents are $a = 1.392, b = 1.258, c = -0.481, d = 0.256, e = -0.115, f = 1.239$ and $g = 0.134$. This is the proposed statistical modeling and ranges are defined for the value of U . Range of U for ‘Normal’ is 1 to 10 and for ‘Diabetic’ it is 11 to 20. Based on the value of U the grading of the disorder can be done.

4. Results and discussion

The training dataset was pre-processed so that it is suitable as an input to the network architecture and the anchor boxes were estimated. The same anchor boxes were used for both YOLOv3 and YOLOv2 network architectures. After training of the models, evaluation was performed on the training dataset itself and then manual evaluation was carried out on the test dataset. Automatic evaluation on the test dataset is not possible as even if the detector detects the classes correctly it might not generate the bounding boxes down to the exact pixel values as that of the bounding boxes labeled manually, which may result in an accuracy of nearly 0%. The performance of both YOLOv2 and YOLOv3 are tabulated in Table 3, and it proves that YOLOv3 outperforms YOLOv2 in terms of average precision.

Table 3. Average precision for each capillary class on the training dataset

Algorithm	Normal	Elongated	Wide	Tortuosity	Hemorrhages
YOLOv3	0.74	0.80	0.85	0.99	0.91
YOLOv2	0.70	0.61	0.74	0.84	0.89

Figure 3 depicts the changes in learning rate and total loss with respect to number of iterations for YOLOv3 architecture. Learning rate increases and converges as number of iterations increase, while total loss decreases.

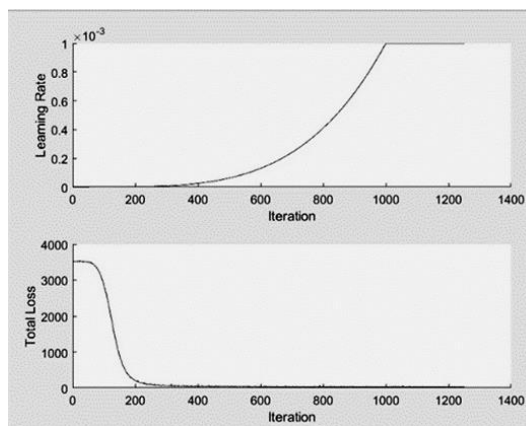


Fig. 3. Learning rate and total loss curves for YOLOv3 architecture

Figure 4 depicts class-wise precision-recall curves. These plots are from the detection algorithm implemented on the training dataset for YOLOv3 architecture. The larger the area under the curve (AUC) the better is the capability to detect that class. Because of the distinct features of tortuous capillaries, it is easiest to detect with an average precision of 0.99. The operating point of the model is set such that the recall of the model is increased at the expense of precision, especially for the Normal class where the AUC is just over 50%. In case of the Normal class, recall is more important than precision as higher recall implies that linear density and avascularity are measured correctly. The average precision values for the other classes are relatively high and satisfactory.

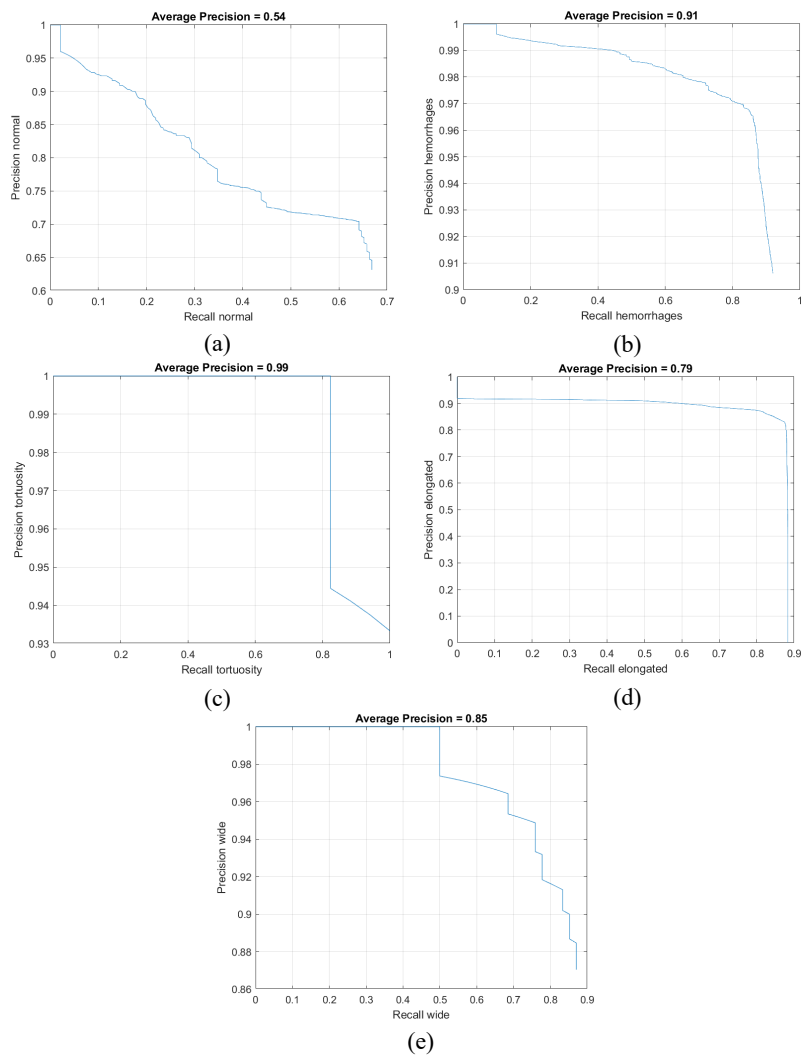


Fig. 4. Precision-recall curves for 5 classes (a) Normal (b) Hemorrhages (c) Tortuosity (d) Elongated (e) Wide

The bounding boxes are displayed around the detected capillaries. Detection capability is depicted by the recall values, while accuracy of detected capillaries is proven by the precision values. The example in Figure 5 displays detection of two abnormal qualitative features i.e., tortuosity and hemorrhages as in Figure 5(d) with the corresponding confidence scores in Figure 5(e). The remaining capillaries are detected to be normal. The quantitative features like width or loop diameter and length of the capillaries are computed and displayed in Figures 5(b) and 5(c). These features are calculated based on distances between capillaries and the dimension of bounding boxes. The distances between the capillaries are 118 μm , 90 μm , 186 μm , 168 μm , 158 μm and 240 μm . In this example, the linear density is 6 capillaries per mm, and the avascularity score is 0 as the distance between any two consecutive capillaries does not exceed 500 μm . The pixel to micron scaling is 1 pixel \approx 2 μm .

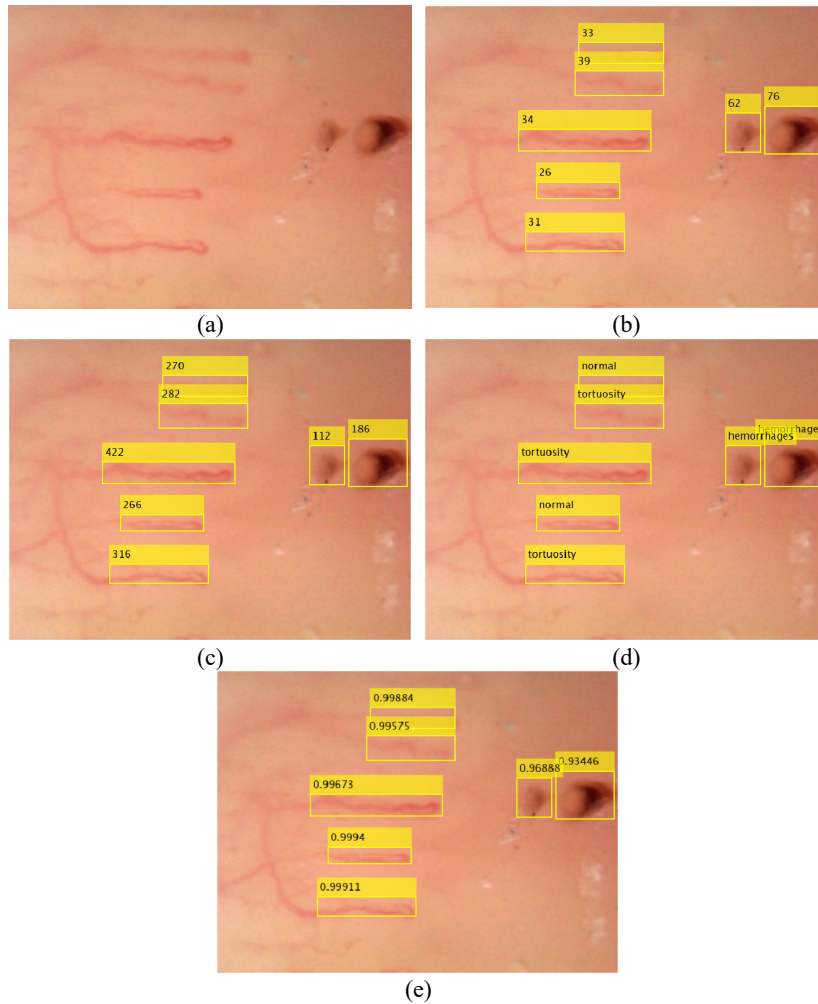


Fig. 5. (a) Raw image (b) Width or loop diameter in μm (c) Length in μm (d) Detected labels (e) Confidence scores

The features extracted are used in the proposed statistical model provided in (1) and (2) and the score U is computed to classify the images as either ‘Normal’ or ‘Diabetic’. Table 4 shows the performance of the model. For the test image dataset of 230 images, the model provided an accuracy of 88.2%, sensitivity of 89% and specificity of 89%. A pilot study conducted earlier by the authors [10], shows the usage of Discrete Cosine Transform (DCT) and Wavelet Transform (WT) for classifying NFC images. The classification accuracy quoted is 73.3%. In comparison, the proposed methodology based on deep learning architectures provides a higher accuracy of 88.2% and therefore is a better model.

Table 4. Performance metrics of the proposed statistical model

Algorithms	Accuracy	Sensitivity	Specificity
Proposed algorithm (based on deep learning)	88.2%	89%	89%
Algorithm based on machine learning [10]	73.3%	71%	75%

Object detection with deep learning approach is employed to acquire the qualitative and quantitative features of capillaries, which aids doctors to evaluate and track the progression of the disorder.

5. Conclusion

The proposed algorithm based on NFC with an USB microscope is a novel and an economically viable approach especially in developing countries. Qualitative features like tortuosity, avascularity, hemorrhages and quantitative features like length of capillaries, loop diameter and capillary density are extracted through deep learning-based object detection algorithm. This would really help doctors to keep a track and evaluate progression of the disorder. The proposed methodology enables detection of diabetes and ensures timely and early treatment to curb the intensification of the disease.

NFC is a technique that has the potential to aid medical practitioners in detecting a wide array of diseases and its utilization can be further expanded to treat RA, hypertension, Reynaud’s disease etc. This model can be modified by incorporating NFC with Artificial Intelligence that can be used for diagnosis of various other micro-vascular diseases. Advanced and sophisticated image processing algorithms can be considered to circumvent the problem of poor contrast which in-turn may improve the detection accuracy.

6. Acknowledgements

We would like to express our gratitude to the Department of Endocrinology, M S Ramaiah Medical Hospital and to Dr. Sudha Tinaikar’s practice at Malleshwaram, Bangalore for making the data collection process possible. We would also like to thank Dr.

Venkatesh of Department of Physiology, Ramaiah Medical College for his valuable inputs in this work.

7. References

- [1] Maldonado G, Paredes C, Roberto G, Ríos C, “Nailfold Capillaroscopy a Non-Invasive Tool for Direct Observation of Microvascular Damage in Diabetes Mellitus: Review”. *JSM Atheroscler*, vol. 2, no. 4, pp. 1037, 2017.
- [2] Jakhar D, Grover C, Singal A, Das GK, Madhu S V, “Nailfold Capillaroscopic Changes in Patients with Type 2 Diabetes Mellitus: An Observational, Comparative Study”, *Indian Journal of Medical Specialties*, vo. 11, pp. 28 – 33, 2020. <https://doi.org/10.4103/INJMS.INJMS.146.19>
- [3] Uyar S, Balkar I A, Erol MK, Yeşil B, Tokuç A, Durmaz D, Görar S, Çekin AH, “Assessment of the Relationship between Diabetic Retinopathy and Nailfold Capillaries in Type 2 Diabetics with a Noninvasive Method: Nailfold Videocapillaroscopy”, *Journal of Diabetes Research*, vol. 2016, 2016. <https://doi.org/10.1155/2016/7592402>
- [4] Berks M, Tresadern P, Dinsdale G, Murray A, Moore T, Herrick A, Taylor C, “An Automated System for Detecting and Measuring Nailfold Capillaries”, *Medical Image Computing and Computer-Assisted Intervention – MICCAI 2014, Lecture Notes in Computer Science*, vol. 8673, pp. 658 – 665, Springer, 2014. https://doi.org/10.1007/978-3-319-10404-1_82
- [5] Suma K. V, Vishwajit Sasi, Bheemsain Rao, “A Novel Approach to Classify Nailfold Capillary Images in Indian Population using USB Digital Microscope”, *International Journal of Biomedical and Clinical Engineering*, vol. 7, no. 1, January – June 2018. <https://doi.org/10.4018/IJBCE.2018010102>
- [6] Mohammed Enamul Hoque, Kuryati Kipli, “Deep Learning in Retinal Image Segmentation and Feature Extraction: A Review,” *International Journal of Online and Biomedical Engineering (iJOE)*, vol. 17, no. 14, pp. 103 – 118, 2021. <https://doi.org/10.3991/ijoe.v17i14.24819>
- [7] Irawati, I. D., Andrea Larasaty, I., & Hadiyoso, S., “Comparison of Convolution Neural Network Architecture for Colon Cancer Classification.” *International Journal of Online and Biomedical Engineering (iJOE)*, vol. 18, no. 3, pp. 164 – 172, 2020. <https://doi.org/10.3991/ijoe.v18i03.27777>
- [8] J. Redmon, A. Farhadi, “YOLO9000: Better, Faster, Stronger”, *Proceedings of the IEEE Conference on Computer Vision and Pattern Recognition (CVPR)*, pp. 7263 – 7271, 2017. <https://doi.org/10.1109/CVPR.2017.690>
- [9] J. Redmon, A. Farhadi, “YOLOv3: An Incremental Improvement”, arXiv: 1804.02767, 2018.
- [10] K. V. Suma, K. Indira and B. Rao, "Classification of Nailfold Capillary Images using Wavelet and Discrete Cosine Transform," *International Conference on Circuits, Communication, Control and Computing*, pp. 105 – 108, 2014. <https://doi.org/10.1109/CIMCA.2014.7057768>

8. Authors

Suma K V, Associate Professor, Department of ECE, Ramaiah Institute of Technology obtained her doctorate for the analysis of nailfold capillary morphology in diabetic and hypertensive patients from Visvesvaraya Technological University (VTU), Belagavi, India in 2019. She completed her B. E from Malnad College of Engineering, Mysore University in 1991 and M. Tech in VLSI Design and Embedded System Design from BMS College of Engineering, Bangalore in 2009. She has numerous publications to her credit in the field of Biomedical Signal/Image Processing, Embedded System Design and Machine Learning. She is an IEEE Senior Member and is Advisor for the IEEE WIE Chapter in Ramaiah Institute of Technology.

S. Sethu Selvi, Professor, Department of ECE, Ramaiah Institute of Technology obtained her Ph. D from Indian Institute of Science in the area of Image Compression. She completed her B. E from Thiagarajar College of Engineering, Madurai in 1992 and M. E from Anna University in 1994. She has numerous publications to her name in the field of Machine Learning, Pattern Recognition and Signal and Image Processing. Her fields of interests are Digital Image Processing, Machine/Deep Learning, Video Processing, Character Recognition and Biometrics. She has authored a chapter titled “Image Algebra and Image Fusion” in the book “Data Fusion Mathematics: Theory and Practice”, CRC Press, 2017 and has been listed as a noteworthy technical contributor by Marquis Who's Who (World), 2009. She is an IEEE Senior Member and is the IEEE SPS Chapter Advisor in Ramaiah Institute of Technology and regularly volunteers for various executive committee positions in IEEE Bangalore Section and IEEE Signal Processing Society Bangalore Chapter.

Pranav Nanda, Manisha Shetty, Vikas M, Kushagra Awasthi are students in the Department of Electronics & Communication, Ramaiah Institute of Technology pursuing their BE course.

Article submitted 2021-10-07. Resubmitted 2022-01-14. Final acceptance 2022-03-14. Final version published as submitted by the authors.